Annualized flash count variations over the US from 2017 through 2023 and their relationship to NLDN algorithms

Martin J. Murphy[i], Vaisala Xweather, Louisville, CO

Kenneth L. Cummins, University of Arizona and Florida Institute of Technology

1. Introduction

Lightning became part of the Global Climate Observing System list of "Essential Climate Variables" (ECV) in 2018 (Aich et al. 2018). An ECV is defined by three key characteristics (Bojinski et al 2014): relevance, feasibility, and cost effectiveness. That is, an ECV must be relevant to describing the climate and climate change, it must be technically feasible to observe the ECV at global scale, and it must be cost effective to observe the ECV globally and provide historical data if possible. Lightning satisfies all three of these characteristics. For many years now, it has been both feasible and cost-effective to observe lightning globally, and relatively long historical lightning data sets exist in many parts of the world. The relevance of lightning to climate has been amply demonstrated in Koshak et al (2015) (section 2), Williams (2005), and references therein: Lightning is expected to be affected by, and to have impacts on, the climate system in a variety of complex ways.

Regarding the impact of climate on lightning, lightning is connected to temperature, water vapor content, and possibly also aerosol concentration, via the dominant process of charge separation in thunderstorms, the non-inductive charge separation mechanism (Baker et al. 1987, Saunders 2008). The world's land masses contain most of the world's thunderstorms given that they are subjected to much larger temperature cycling than the ocean surfaces (Williams and Stanfill, 2002). As described in Williams (2005), lightning is obviously responsive to temperature on the diurnal time scale, with lightning maxima occurring over the major land masses in the local afternoon (mostly) after each land mass is successively rotated in front of the sun and warmed. On the annual time scale, lightning peaks during the northern hemisphere summer because the northern hemisphere contains much more of the land mass than the southern hemisphere. The combined role of water vapor and temperature has been shown to be important via the depth of the dry boundary layer (see Williams and Stanfill, 2002): a deeper dry boundary layer requires larger thermals to reach the lifting condensation level; larger thermals are less subject to mix-out of cloud droplets above cloud base, assuming that the boundary layer is not so dry as to prevent cloud formation completely. Aerosol has been thought to play a role insofar as a relatively clean boundary layer is thought to lead to more of the warm rain process via the collision-coalescence of larger droplets, and thus less ice in the mid-troposphere, and thus less charge separation (Williams et al 2002; Stolz et al., 2017; Wang et al., 2018). The possible role of aerosol has received renewed attention lately in light of the covid pandemic (Liu et al. 2024, submitted), illustrating the complexity of separating background decadal variations from short-term aerosol effects. Earlier studies (summarized in Williams 2005) indicated that thermodynamic factors were generally more important, although more recent work (see Williams 2020 and references therein) suggests that aerosol and thermodynamic contributions may be comparable under certain conditions.

As noted above, observations of lightning have been available from ground-based networks of radio-frequency receivers ("lightning locating systems", or LLSs), in some cases covering large territories for long periods of time (e.g. Cummins et al. 1998; Cummins and Murphy, 2009; Zhu et al., 2021). Long-range VLF receiver networks such as WWLLN (Hutchins et al. 2012) and GLD360 (Said, 2017) cover the entire planet and by now have their own fairly long data archives. Since the late 2010s, continuous observations of lightning from geostationary orbit are also available over the western hemisphere from the two GOES satellites (Rudlosky et al. 2020), and in China and the Pacific Rim in the warm season (Zhi et al., 2024). In the near future, similar observations will also become routinely available over the rest of the eastern hemisphere as well (Holmund et al. 2021).

Of course, all observing systems have biases that need to be addressed in order to make sense of long histories of observations. In the case of LLSs, one of the most relevant issues is the fraction of detected lightning (a.k.a. detection efficiency or DE), which changes over time as a result of improvements in sensing capability and/or increases in the number of deployed sensors. A method of determining DE corrections in LLS data was provided by Medici et al. (2017). DE variations can also be managed without actually correcting them by using thunderstorm hour counts instead of lightning event or flash counts (Bourscheidt et al. 2012; DiGangi et al. 2022). Another important issue with LLS data is in how lightning events are classified by type (cloud-to-ground, CG, vs cloud, IC). Changes in the type classification algorithm in the U.S. National Lightning Detection Network (NLDN) and simple means of normalizing the classifications of data from different years / system upgrades are documented in Murphy et al. (2021a,b).

In this paper, we present spatial and temporal analyses of seven full years of CG and total (IC+CG) flash data over the continental US (CONUS), 2017 through 2023, and the anomalies between each year and the seven-year average. We process all lightning data from the NLDN using two different type classification algorithms, and we further demonstrate that as long as the same classification is applied to all data, the 2017-2023 trend does not depend on the classification method. Further, we show that the application of the simple reclassification method (Murphy et al. 2021b) leads to a change of a few percent relative to the use of the full classification algorithm. Finally, we compare the lightning anomalies over the seven-year period to anomalies of relevant meteorological variables using the PRISM (Daly et al. 2008) surface and NARR (Mesinger et al. 2006) upper air data sets: 2-m temperature, 2-m dew point, and surface precipitation (PRISM) and CAPE and CIN (NARR) over the main thunderstorm season months of May through September.

2. Classification and flash clustering

The majority of results in this paper are determined by reprocessing all older NLDN data with the currently operational type classification algorithm discussed by Murphy et al. (2021b); to avoid confusion, this algorithm is hereafter called the "2021-onward" algorithm because it went into production in late May, 2021. Given that, the first 4.5 years (approximately) of the data in this study had to be reprocessed, with all later data used as is. In addition, we reprocessed all seven years of data using the type classification algorithm that had been operational prior to 2015 (including the reclassification of all positive events < 15 kA as ICs), when effectively only a single measure of the waveform shape was made available to the central processing system in an older data format coming from the sensors. Finally, we reprocessed the 2020 and 2023 data using the approximate classification normalization method given in Murphy et al. (2021b). This method is intended to mimic the 2021-onward classification algorithm and is applicable to data sets back as far as 1995; we show the sensitivity of the mimicked classification relative to the full 2021-onward classification.

Flash clustering is done using the algorithm given in Murphy et al. (2021a) because it takes into account the fact that IC pulses often occur as part of CG flashes due to preliminary breakdown or K processes during inter-stroke intervals. In flash-level analysis, such as this study, any flash having at least one CG stroke is a CG flash and is represented by the position (and polarity and peak current) of its first return stroke. All other flashes are IC flashes and are represented by their first IC pulses. Flash counts are accumulated on a 0.5-degree lat, lon grid. Both CG and total ("TL") flash counts by grid box per year and their anomalies are presented. Anomalies are determined with respect to the seven-year average.

3. Results – lightning counts and anomalies

Figure 1 shows the seven-year average CG (left) and total lightning (TL, right) flash counts on 0.5 X 0.5 degree grids and on logarithmic color scales. The usual patterns found in other US lightning climatologies are evident here. The maximum is in Florida, but of course, high values extend westward along the Gulf coast and up into the south-central US. The southwest US / northwestern Mexico and the Gulf stream off the southeast coast are secondary local maxima. The absolute minimum is along the west coast, and the Appalachian mountains

exhibit a local minimum. The fall-off of flash density with increasing distance outside the US in the Atlantic, Pacific, and to the south is the result of decreasing flash DE, which is somewhat more rapid for total lightning.

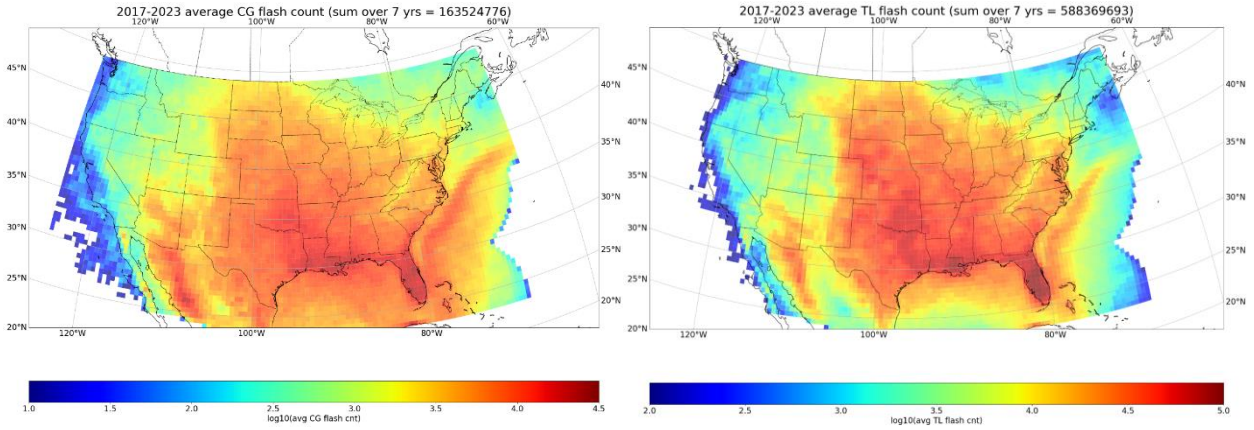


*Figure 1. Average flash counts on 0.5*0.5 degree grid over seven-year period of analysis using the 2021-onward classification algorithm: Left = CG, right = TL. Both on log scales with CG scale ranging 1 – 4.5 (10 – 32000 / grid box) and TL scale ranging 2 – 5 (100 – 100000 / grid box)*

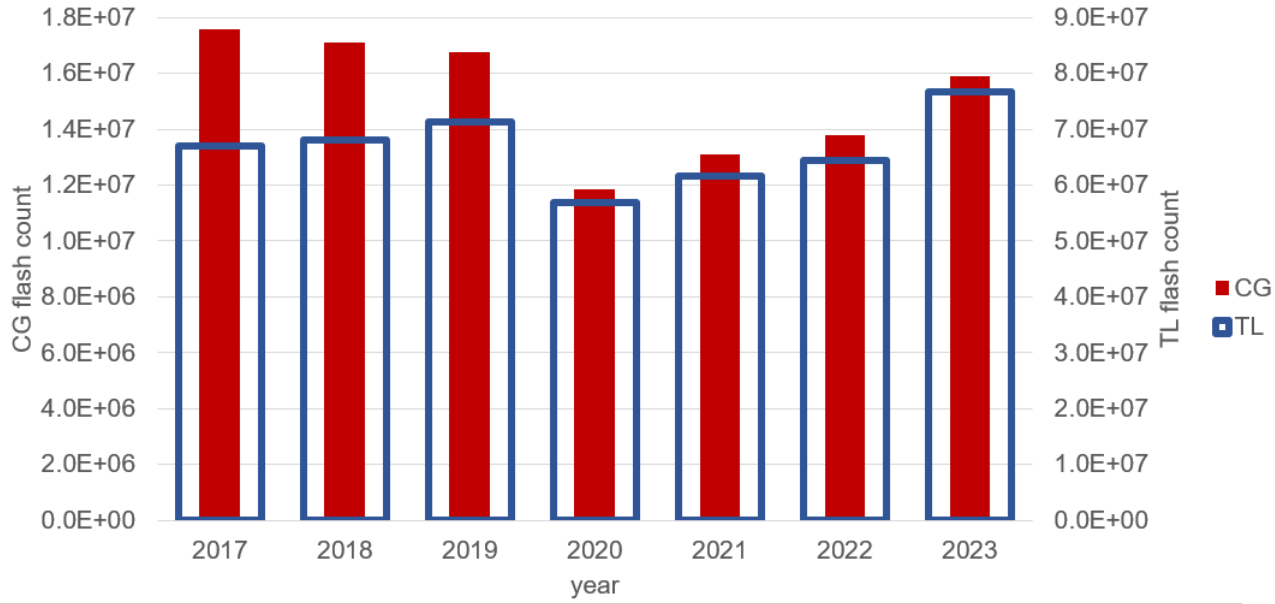


Figure 2. CG flash count (left axis, solid red bars) and TL flash count (right axis, open blue bars) per year over the seven years of data using the 2021-onward classification.

Figure 2 shows the annual counts of CG (solid red bars) and TL (open blue bars) over all of CONUS per year within the seven-year data set. In both CG and TL flashes, 2020 was a remarkable minimum and was followed by a slow recovery through 2023. Prior to 2020, CG flashes peaked in 2017 and declined very slowly, whereas TL flashes increased slowly through 2019. Notice also that TL flashes reached a maximum in 2023 whereas CG flashes in 2023 were still somewhat lower than in 2017-19. This shows that the overall IC-CG flash ratio crept slowly upward over the seven-year period, which is a potentially interesting topic of future research, and we note also that this is not due to any change in sensor or network sensitivity.

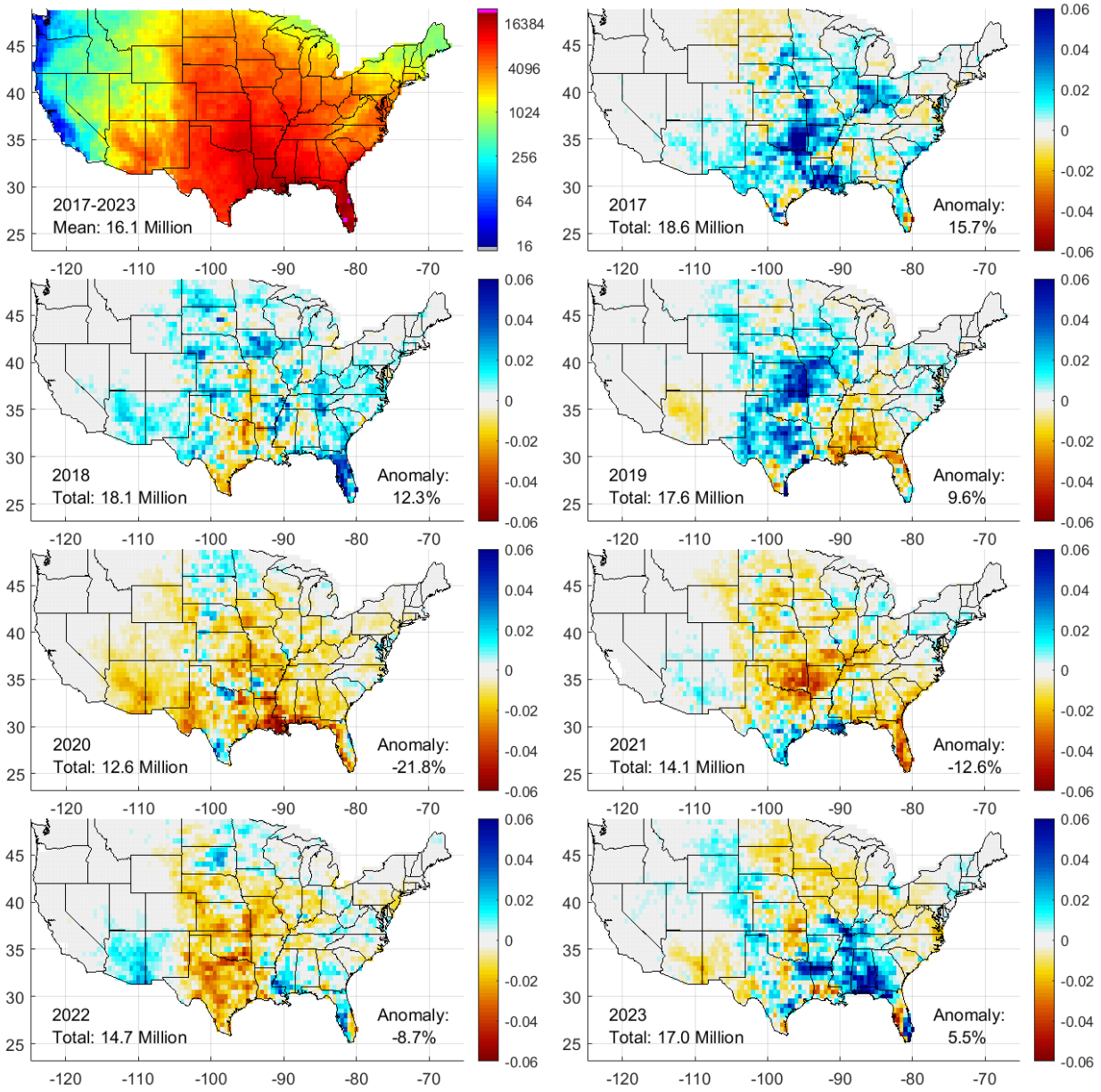


Figure 3. Top left: average annual CG flash count on 0.5 X 0.5 degree grid. Remaining panels show 2017-2023 contributions to annual anomaly in CG using the 2021-onward classification.

In figure 3, we map the contributions to the total annual CG flash anomalies spatially over the US on a per-year basis. The contribution from each 0.5 X 0.5 degree grid box is determined by dividing the anomaly in CG flash count by the average number of full-CONUS flashes over the seven years, such that the sum over all grid boxes yields the total annual flash count anomaly for a given year. That total annual anomaly value is given as a percentage in the lower right corner of each panel of figure 3. Figure 4 shows the total lightning flash count anomalies in the same format. By showing contributions to the total anomaly, the grid boxes that contribute most to the total appear in the strongest colors. For example, while most of the interior west experienced large negative anomalies in 2020 relative to the normal amount of lightning in those areas, the contribution to the total from the interior west is relatively insignificant because relatively little of the lightning occurs there,

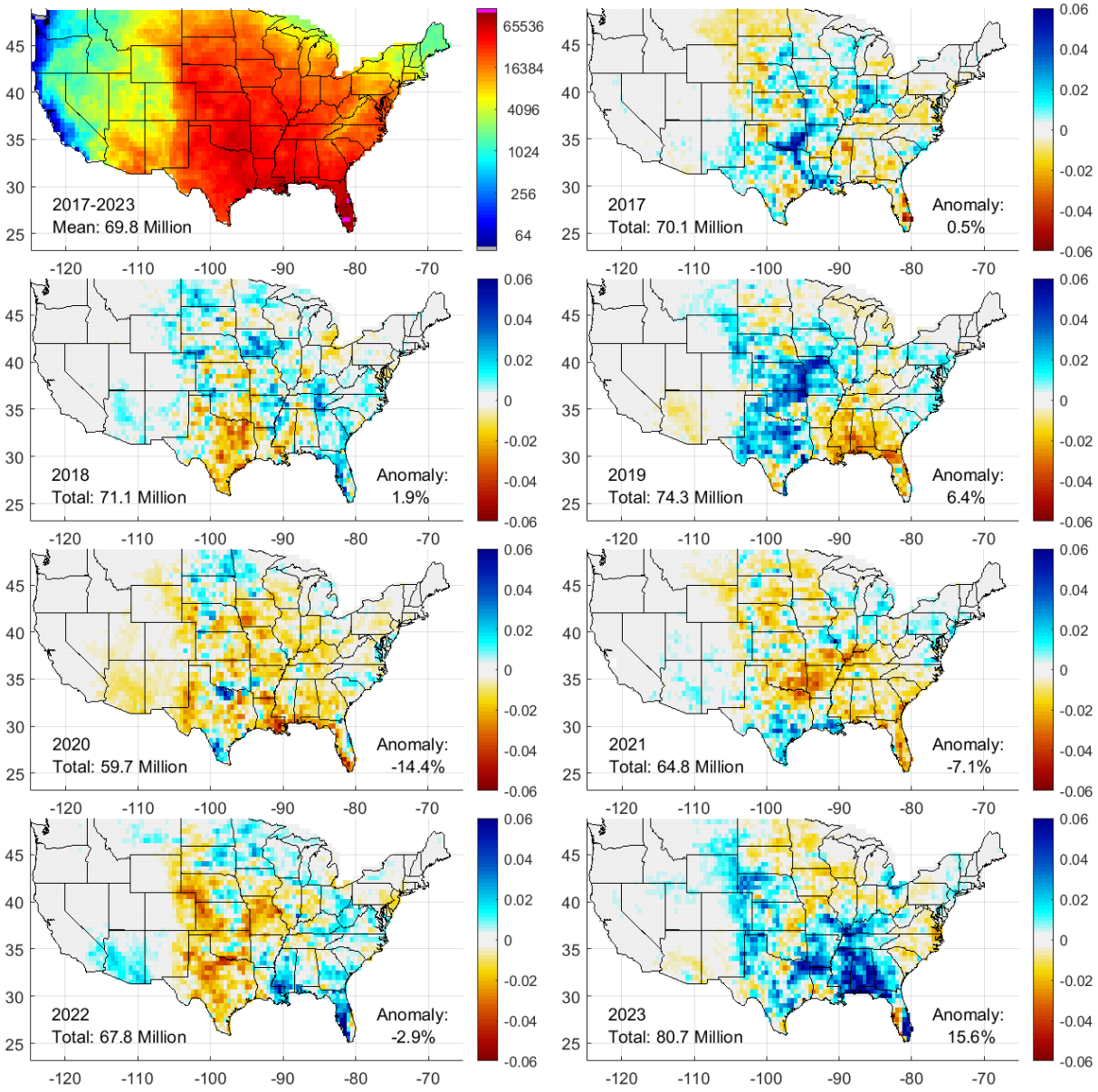


Figure 4. Top left: average annual total lightning count on 0.5 X 0.5 degree grid. Remaining panels show 2017-2023 contributions to annual anomaly in TL using the 2021-onward classification.

outside of the southwestern summer monsoon region. In the various panels of figures 3 and 4, we see intricate spatial patterns of anomaly contributions across the various years. To some extent, we need to beware of statistical noise: we note that in 2020, a patch of northern Texas had positive anomalies but was completely surrounded by the negative anomalies that reigned over most of the US. It turns out that a single day produced 17.3% of all flashes observed in 2020 in that patch of north Texas, whereas in 2017 (when anomalies were also positive) the biggest single day produced only 8.1% of all flashes in that same area. So even on 0.5-degree grids, we have to be careful not to over-interpret small-scale anomalies. However, broad, interesting spatial patterns are clearly evident and variable from year to year. For example, in the lightning-dominant regions of the country, the central and southern plains, Gulf coast, and southeast, the patterns of anomalies between

2019 and 2022 are nearly mirror images of each other. In 2019, the plains had strong positive anomalies whereas the southeast (and southwest, to a lesser extent) were negative, while in 2022, the plains were negative but the southeast and southwest were mostly positive.

As discussed in the next section, the trends are robust against variations in the lightning type classification algorithm provided that the same algorithm or normalization method is applied to all years. That of course means that there are interesting and important real variations in lightning over these seven years. Following the discussion of classification algorithms, we then start to examine some potential factors behind these real variations in lightning.

4. Results – sensitivity to classification

Figure 5 shows the annual CG flash counts using the pre-2015 classification algorithm (blue, solid) and 2021-onward classification (red, hatched). In addition, the two lines show the percent of average, with the average taken over the seven-year period. The 2021-onward classification algorithm produces fewer CG flashes than the pre-2015 algorithm, primarily due to the reclassification of a population of low-current negative "CG" strokes into the IC class (Murphy et al. 2021b). The trend over the seven-year period, however, is very well captured by both algorithms, showing differences of less than 2% between the two. Though not shown here, spatial patterns of lightning anomalies are also consistent regardless of which classification algorithm is used, as long as the same classification is applied to all years.

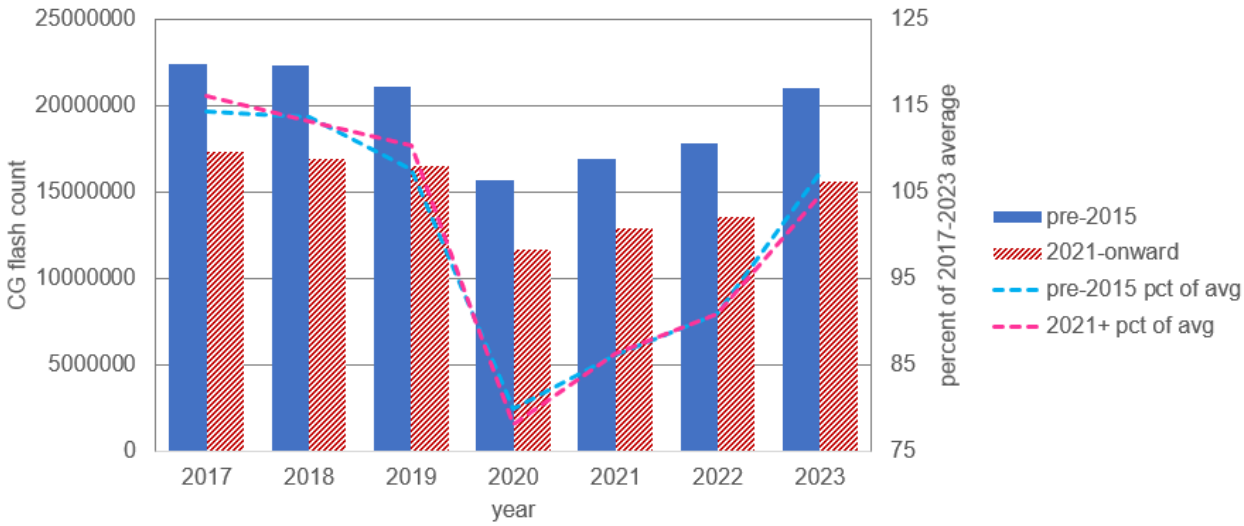


Figure 5. CG flash counts (bars, left axis) using the pre-2015 (blue, solid bars) and 2021-onward (red, hatched bars) classification algorithms. Dashed lines show the percentage of the 2017-2023 average and refer to the right axis.

In order to facilitate the normalization of classifications across years, and thus facilitate long-term climatological study, Murphy et al. 2021b presented simple two-parameter linear regressions (one applicable to negative events, the other to positives). These establish linear classification boundaries based on two commonly available values, peak current (signed) and peak-to-zero time. The objective is to replicate as closely as possible the 2021-onward classification algorithm but with two widely available (back to 1995), accessible data values. In this study, we have applied that linear regression method to the 2020 and 2023 data sets. Note that the objective of the linear regression is to reproduce the 2021-onward type classification, and thus the 2020 data set had to be reprocessed, as described in section 2 above. Relative to the 2021-onward

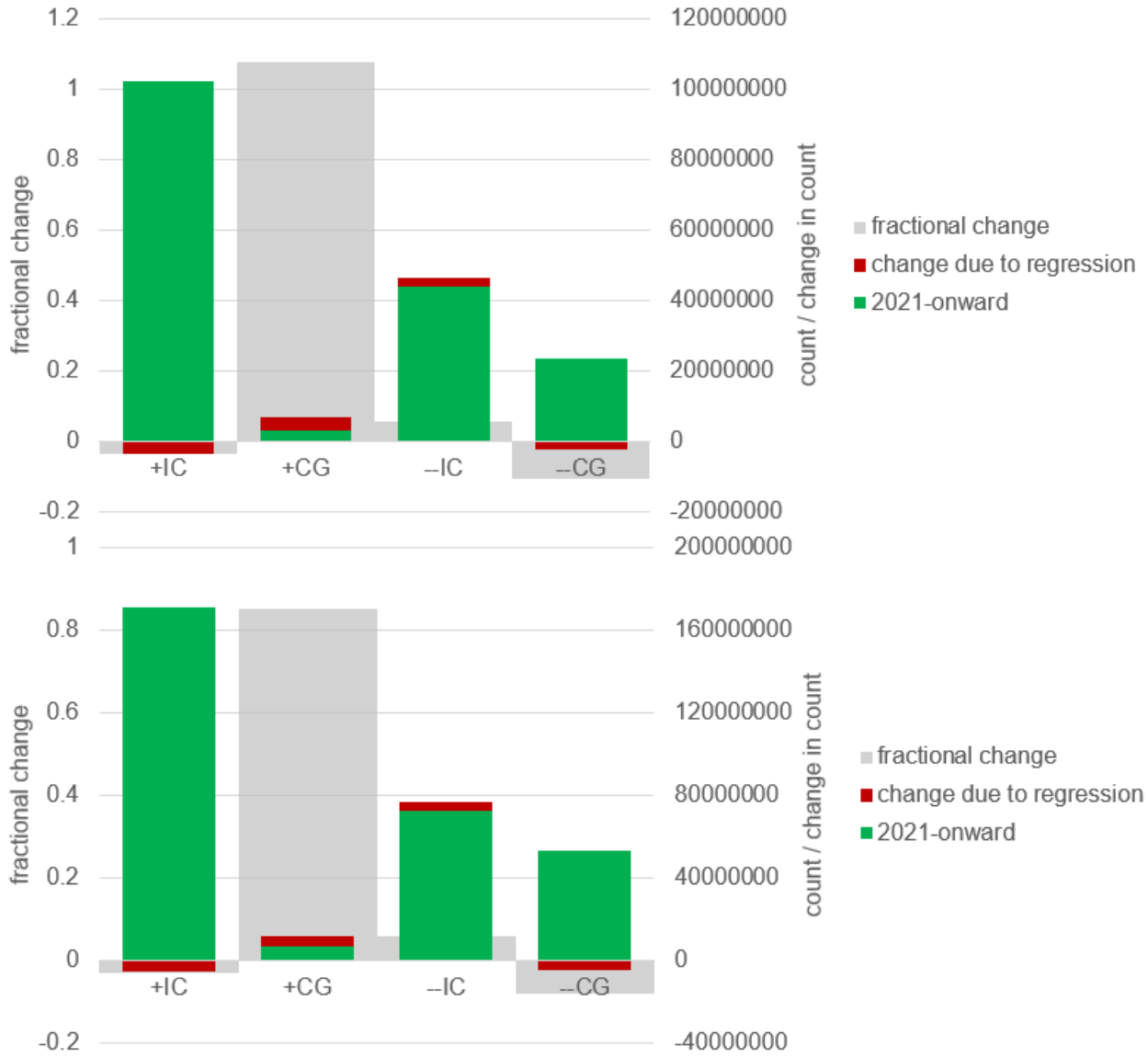


Figure 6. Comparison of the 2021-onward classification algorithm with the simple 2-parameter linear regression given in Murphy et al. 2021b. Absolute counts from the 2021-onward algorithm are given in green, with respect to the right-hand axis. The changes in absolute count are in red, also with respect to the right-hand axis (stacked on the green bars), and the fractional change of each type is in gray, with respect to the left-hand axis. Top = 2020, bottom = 2023.

classification algorithm, the linear regression faithfully reproduces the classification of 96.5% of all 2020 events and 96.8% of all 2023 events; the overall percentages reclassified are 3.5% in 2020 and 3.2% in 2023. This is consistent with the overall reclassification rate that we found in 2021 (Murphy et al., 2021b): 3.8 to 5.5%, depending on which of the older algorithms we started from. By individual lightning type (+IC, –IC, +CG, and –CG), the percent changes are, not surprisingly, very different. Figure 6 shows the absolute counts of each type using the 2021-onward classification method (green bars), the change in count due to the 2-parameter linear regression (red bars stacked on the green), and the fractional change in each type due to the linear regression relative to the 2021-onward classification (pale gray bars). Both 2020 (top) and 2023 (bottom) are shown, and both have exactly the same pattern of behavior. Positive polarity IC events outnumber +CG strokes by a factor of 25-30, so even though a small absolute number of +IC events is reclassified as +CG by the linear regression,

that small absolute number roughly doubles the number of +CG strokes. On the negative polarity side, 8 – 10% of negative CG strokes are reclassified as –IC pulses by the linear regression.

5. Results / discussion – comparison against meteorological variables

As an introduction to the question of relating the lightning behavior to the meteorological behavior over our seven-year analysis period, figure 7 presents some common meteorological variables that have been used in comparisons with lightning and possible changes in lightning in the future (e.g. Romps et al. 2014, 2018; Williams 2020). Figure 7 is directly comparable with the dotted lines in figure 5 above, with each annual value expressed as a percent of its seven-year average value. The top section shows three surface variables: precipitation, 2-m dew point, and 2-m temperature, and the bottom section shows two upper air quantities, CAPE and CIN, as well as their sum. We note that 2020 was generally low, but not the lowest in surface

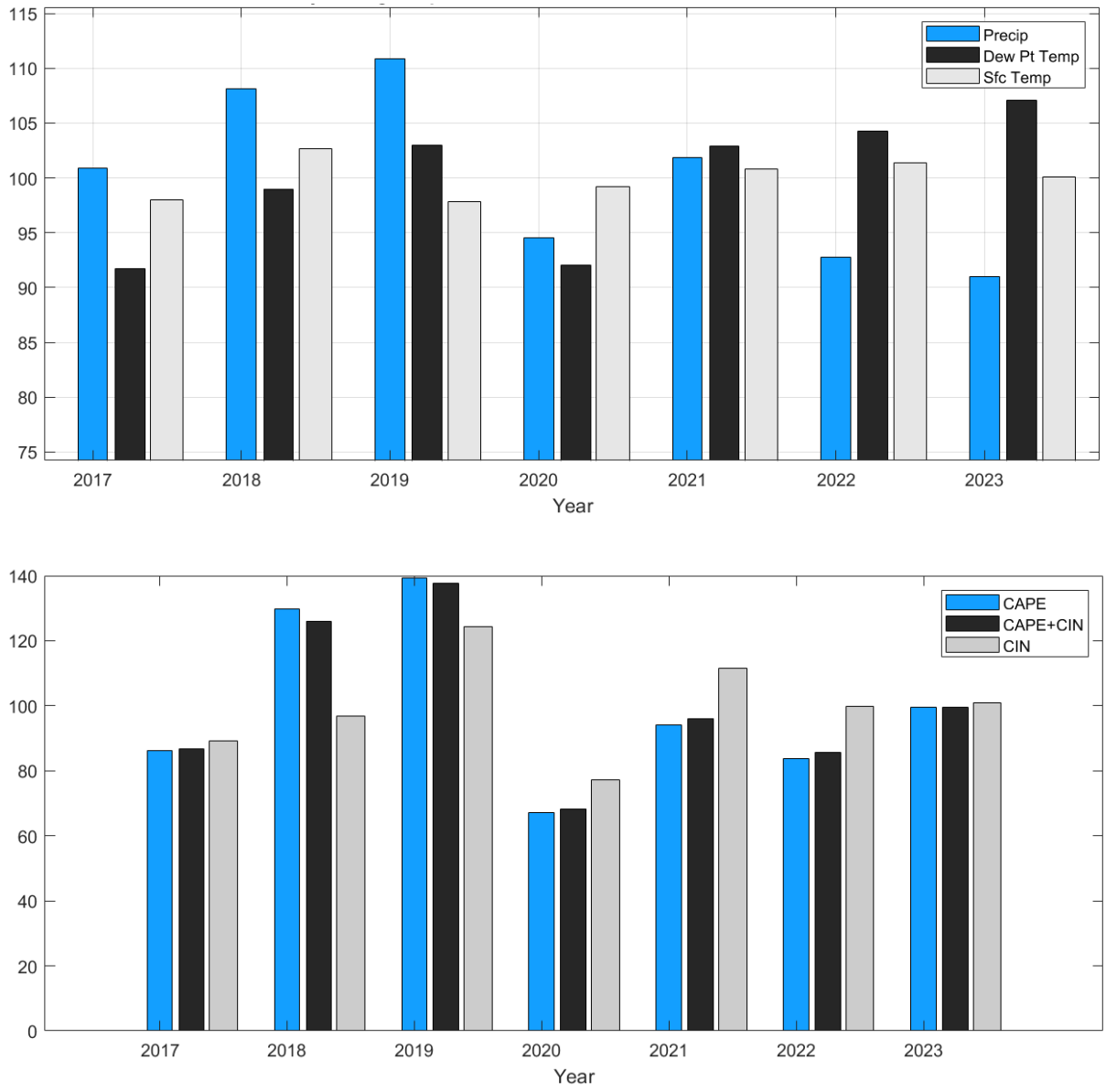


Figure 7. Surface meteorological variables (top) and upper air variables (bottom). All are expressed as percent of average, with average taken over the seven-year period of analysis.

precipitation or surface temperature. None of the temporal patterns in the meteorological variables exactly matches the pattern of CG flashes in figure 2, although the dew point temperature trend is the closest to matching the trend in total flashes in figure 2.

To illustrate the complexity of relationships between meteorological observations routinely taken at the surface and lightning, a comparison of 2017 and 2020 is instructive because they had the highest and lowest CG flash counts. Figure 8 presents the 2017 maps of the CG and TL anomalies relative to the seven-year average together with maps of the anomalies of 2-m dew point and 2-m temperature during the warm-season months of May through September. Figure 9 presents the same maps from 2020. The contrast in lightning between the two years is very stark: 2020 was a very anomalously low lightning year, dominated by the Gulf coast states but additionally heavily influenced by low lightning amounts in the Great Plains and southwest, whereas 2017 had a large positive anomaly in lightning counts, especially over the southern Plains and southern Great Lakes / Ohio valley. Yet, when we look at anomalies of dew point and surface temperatures, we see that both 2017 and 2020 were below the seven-year average, but 2017 was *more* below average than 2020, especially in the dominant lightning-producing regions east of the Rockies and south of the Great Lakes. In other words, surface-based drivers of general thunderstorm activity cannot fully explain the lightning anomalies. Invoking aerosol as an explanation is similarly problematic: although the general theme of Liu et al. (2024) is that the reduction of aerosol in most parts of the world in 2020 as a result of covid is linked to a reduction in lightning, they actually show that most of the central and southern Great Plains of the US were somewhat above average in aerosol optical depth, not below. Yet, most of those areas had below-average amounts of lightning in 2020.

Just as the surface meteorological variables do not yield any straightforward relationships with the lightning behavior, neither do the vertical profile variables CAPE and CIN. Figure 10 shows the anomalies of CAPE and

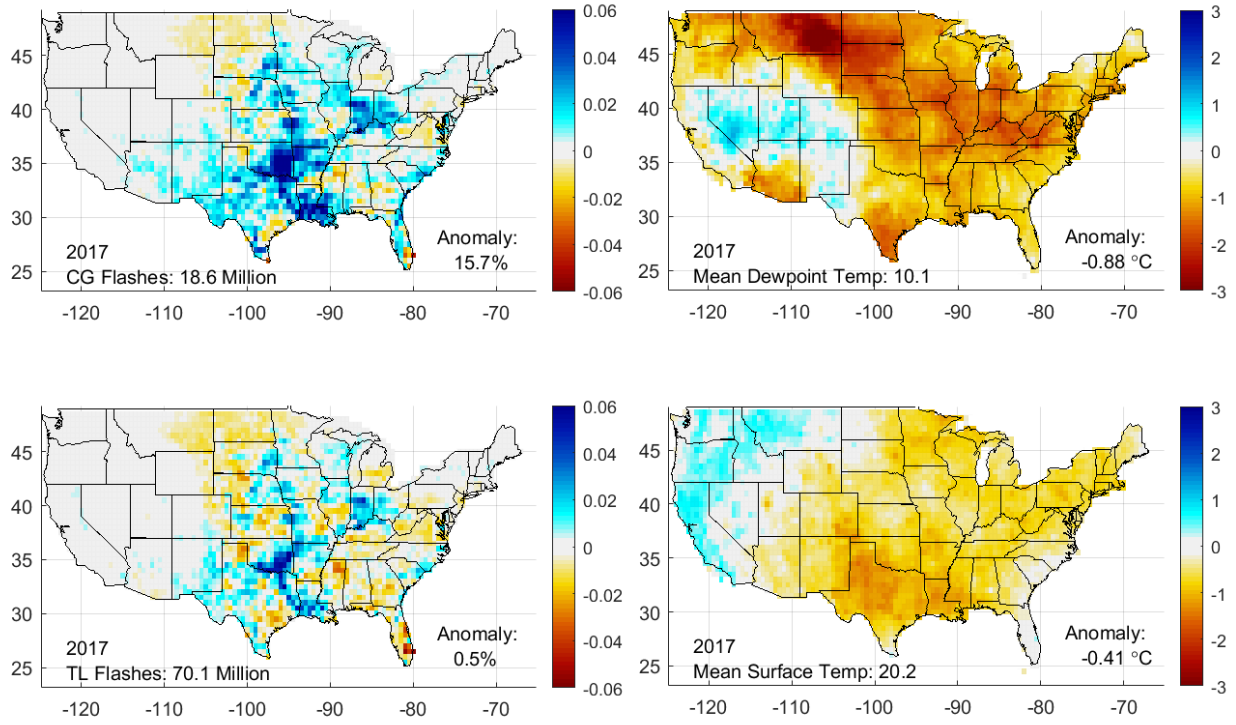


Figure 8. 2017 anomaly maps of CG flashes (top left) and TL flashes (bottom left), and anomaly maps of surface dew point temperature in degrees C (top right) and surface temperature (bottom right) during the warm season.

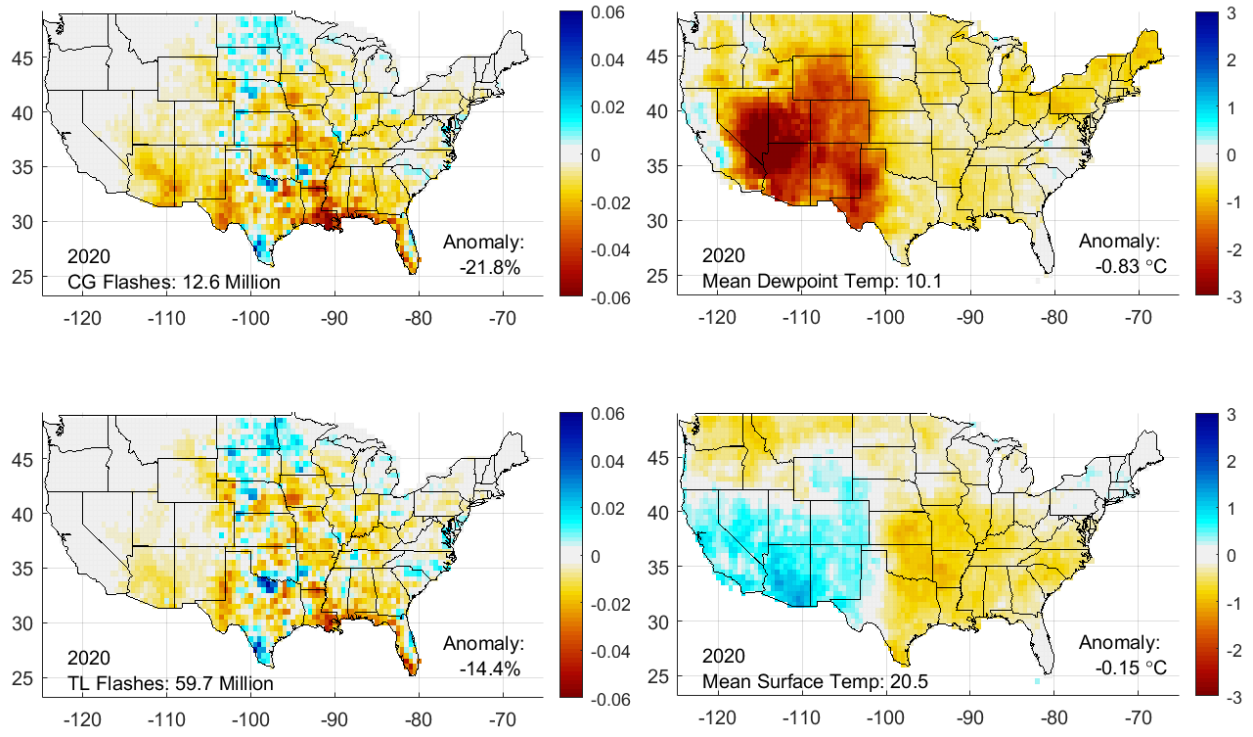


Figure 9. 2020 anomaly maps in same format as figure 8.

CIN in J/kg in 2017 (top) and 2020 (bottom). In both years, CAPE was below average over most areas from the Great Plains to the east coast, although it was obviously more below average in 2020. CIN, however, was also below average; note that CIN is a negative number, so positive anomalies indicate that less CIN was present relative to the seven-year average. From the Great Plains eastward, CIN was below average in most places in both years, even though 2017 had significantly positive lightning anomalies while 2020 was significantly negative.

The lack of clear relationships between the temporal and spatial patterns of lightning anomalies and those of the surface and upper air meteorological variables suggests that temporal aggregation over entire warm seasons probably hides the actual relationships. Tippett and Koshak (2018) and Romps et al. (2018) have shown that daily and sub-daily values, even when aggregated spatially over the US, do show clear relationships between lightning and bulk variables (in their case, the product of CAPE and precipitation rate) that are expected to be generally useful as proxies of lightning. Our preliminary comparisons of 2017 and 2020 using daily values of lightning, the CAPE-precipitation product, and CAPE also suggest a clearer relationship on the daily scale, and further suggest that spring lightning in 2017 with moderate CAPE contributed more to the difference between 2017 and 2020 than mid-summer lightning. Further detailed study is definitely warranted.

Figure 11 presents a different view of some of the complexity, using just the 2020 data because it was the most extreme lightning anomaly year. The scatter plots on the top tier of figure 11 are obtained from the individual grid boxes in the 0.5 X 0.5 degree gridded data set. The x and y variables in both scatter plots are warm-season average dew point (x axis) and surface temperature (y axis), both in degrees C, from the PRISM data set (Daly et al. 2008). The dotted lines in the scatter plots represent a dew point depression of 10 C, corresponding roughly to a cloud base height of 1.25 km using the simple relationship provided by Lawrence (2005). Color in the upper

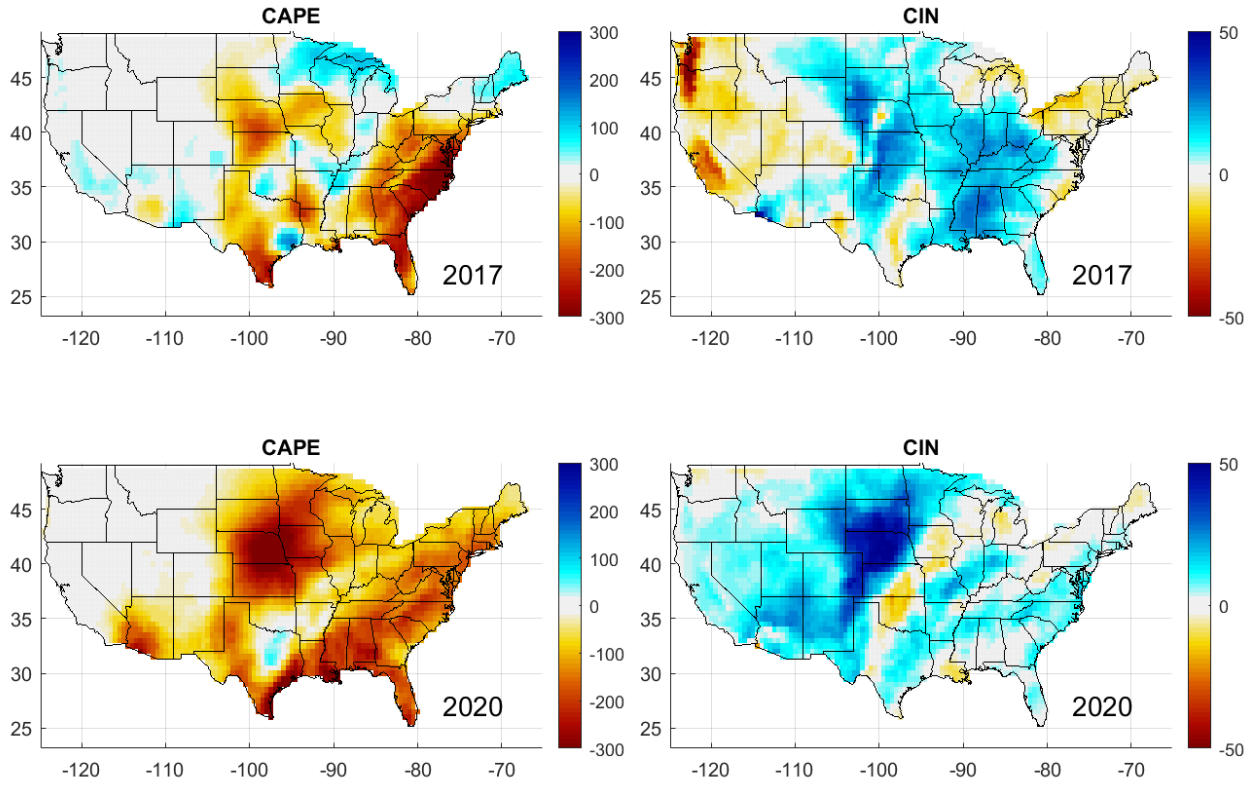


Figure 10. Anomalies of CAPE (left) and CIN (right) in J/kg, relative to the seven-year average. Top is 2017, bottom is 2020.

left plot represents the number of CG flashes, while in the upper right plot, color represents warm-season precipitation (also from PRISM; mm, monthly). CG flashes generically tend to increase as dew point and surface temperature increase, but not with the same behavior as precipitation. CG flash counts generally favor higher cloud base heights: they were high in some of the relatively drier environments where precipitation was relatively low (e.g. dew point between 10 – 17 C with surface temperature between 20 – 25 C). These are presumably in some areas of the high plains and south Texas where relatively high CG counts are seen. Conversely, precipitation was high and CG flash counts notably low in regions of higher dew points but only slightly lower surface temperature; the mid-Atlantic coastal region is particularly notable in this regard. Figure 11 reinforces the fact that long-term averages of surface-based drivers of convective instability and thunderstorm activity in general cannot fully explain the lightning anomalies.

6. Discussion

The seven-year period of our investigation features significant interannual variability alongside significant spatial variability among many of the considered years. These patterns are not readily explained by comparison with either surface or upper air meteorological information, at least not when aggregated over entire warm seasons.

The relationships between major interannual and sub-seasonal climate indices and lightning over the US have been investigated in a number of studies. For example, Koehler (2020) found that annual averages of the Southern Oscillation Index (SOI, related to the El Niño Southern Oscillation, ENSO, cycle) and Pacific Decadal Oscillation (PDO) Index correlate with variations in thunderstorm days over the US. Spatial patterns of variations in thunderstorm days were also shown in that study over five-year periods, but they differ from the

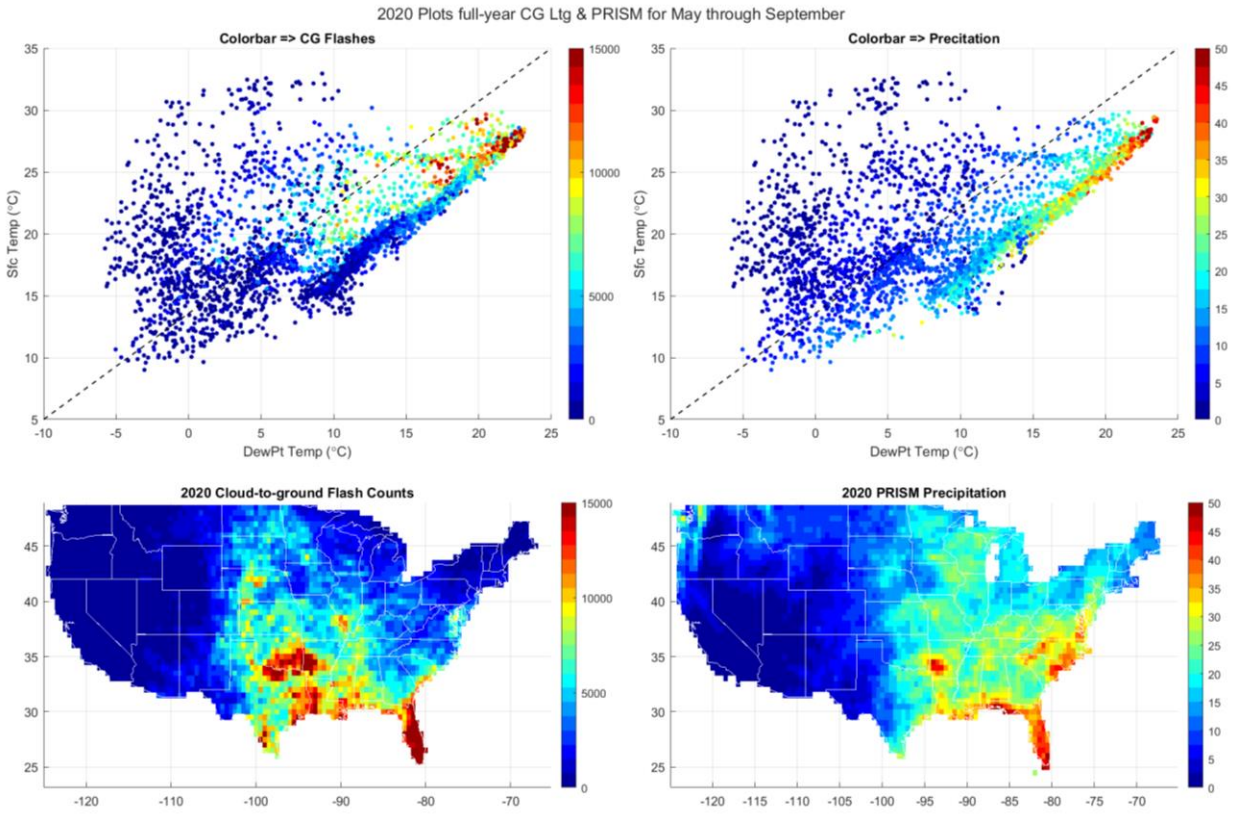


*Figure 11. Top: scatter plots of surface temperature vs. dew point (both in degrees C) in 2020, color coded by the amount of CG flashes (on a 0.5 * 0.5 degree grid) in the upper left, and by precipitation (mm) in the upper right. Temperature, dew point, and precipitation from the PRISM data set (Daly et al. 2008). Bottom: maps of CG flashes (bottom left) and precipitation (bottom right) in 2020.*

spatial patterns of anomalies that we observe in our year-to-year variations (figures 3,4). Malloy et al. (2023) looked at the Oceanic Niño Index (ONI) and the sub-seasonal Madden-Julian Oscillation with respect to US lightning between 2003-2016. In some parts of the US that have significant lightning activity, the ONI has some significant relationship to lightning in the cold season, but none of the lightning-dominant regions of the US shows a significant relationship with ONI during the summer months when most of the lightning actually occurs. Spatially, Malloy et al. show an interesting dipole of positive vs negative correlations of ONI and lightning between the southwest US and the mid-Mississippi region, but again, not applicable to the warm season. Malloy et al found no relationship between the MJO and warm-season lightning either. The interference pattern between ENSO and the PDO is discussed by Kurtzman and Scanlon (2007). Although their primary focus is winter precipitation in areas of the US that experience wet El Niño winters, they also show maps of the difference in spatial pattern between areas that experience warm-phase reinforcement between ENSO and PDO and areas that experience cold-phase reinforcement. That spatial pattern has an interesting wavelength that looks similar to some of the interannual spatial variability that we see in our figures 3 and 4 and suggests a possible avenue of future investigation of the lightning variability.

On longer time scales, Taszarek et al. (2021) highlighted the importance of trends in CIN. Over the US between 1979 and 2019, they find a significant increase in CIN from the high plains eastward, covering precisely the areas where most lightning occurs. The increase in CIN partially overlaps with an extensive area of the interior west and central US where the low-level relative humidity has trended downward. Overall, the end result appears to be an increase in the fraction of environments with |CIN| > 75 J/kg out of all environments with CAPE

> 150 J/kg. Such environments limit convective initiation, leading to a general decrease in thunderstorms. Another long-term effect that should affect lightning is the potential reduction in the efficiency of conversion of CAPE to kinetic energy in a warmer atmosphere due to increased dilution by entrainment (Peters et al. 2024).

7. Future work

This study shows that there are interesting and important interannual and spatial variations in lightning activity over the continental US. Finer subdivision in time appears to be necessary, however, as indicated by the good explanatory power of bulk properties such as the CAPE-precipitation product on the daily and sub-daily time scales (Tippett and Koshak 2018; Romps et al. 2018).

The relationship between the interannual variations of lightning and global interannual climate cycles such as ENSO and PDO merits further study. Tying the results of this study together with the pre-2013 period examined by Koshak et al. (2015) is also worth pursuing. That would enable a much richer investigation of the relationship with interannual climate cycles but also provide much-needed evidence of any longer-term trend that may exist, and its direction. Such a study would necessarily avail itself of the CG detection efficiency correction capability given by Medici et al. (2017) for years prior to 2013. The ability to reprocess data using the pre-2015 lightning type classification, or otherwise normalize across classification algorithm changes, in order to minimize algorithm-based artifacts in CG flash count variations is also important in extending to pre-2015 data sets.

References

Aich, V., Holzworth, R., Goodman, S.J., Kuleshov, Y., Price, C., and Williams, E., 2018: Lightning: A new essential climate variable, *Eos*, **99**, https://doi.org/10.1029/2018EO104583

Bojinski, S., Verstraete, M., Peterson, T.C., Richter, C., Simmons, A., and Zemp, M., 2014: The concept of essential climate variables in support of climate research, applications, and policy, *Bull. Amer. Meteorol. Soc.*, **95**, 1431-1443, https://doi.org/10.1175/BAMS-D-13-00047.1

Bourscheidt, V., Cummins, K.L., Pinto Jr., O., and Naccarato, K.P., 2012: Methods to overcome lightning location system performance limitations on spatial and temporal analysis: Brazilian case, *J. Atmos. Ocean. Tech.*, **29**, 1304-1311, doi:10.1175/JTECH-D-11-00213.1

Cummins, K.L., Murphy, M.J., Bardo, E.A., Hiscox, W.L., Pyle, R.B., and Pifer, A.E., 1998: A combined TOA/MDF technology upgrade of the U.S. National Lightning Detection Network, *J. Geophys. Res.*, **103**, 9035-9044.

Cummins, K.L. and Murphy, M.J., 2009: An overview of lightning locating systems: History, techniques, and data uses, with an in-depth look at the US NLDN, *IEEE Trans. Electromag. Compat.*, **51**, 499-518.

Daly, C., Halbleib, M., Smith, J.I., Gibson, W.P., Doggett, M.K., Taylor, G.H., Curtis, J. and Pasteris, P.P., 2008: Physiographically sensitive mapping of climatological temperature and precipitation across the conterminous United States. *Int. J. Climatol.*, **28**, 2031–2064, https://doi.org/10.1002/joc.1688

DiGangi, E.A., Stock, M., and LaPierre, J., 2022: Thunder hours: How old methods offer new insights into thunderstorm climatology, *Bull. Amer. Meteorol. Soc.*, **103**, https://doi.org/10.1175/BAMS-D-20-0198.1

Holmund, K., Grandell, J., et al, 2021: Meteosat Third Generation (MTG): Continuation and innovation of observations from geostationary orbit, *Bull. Amer. Meteorol. Soc.*, **102**, https://doi.org/10.1175/BAMS-D-19-0304.1

Hutchins, M.L., Holzworth, R.H., Brundell, J.B., and Rodger, C.J., 2012: Relative detection efficiency of the World Wide Lightning Location Network. *Radio Sci.*, **47**, RS6005. https://doi.org/10.1029/2012RS005049

Koehler, T.L., 2020: Cloud-to-ground lightning flash density and thunderstorm day distributions over the contiguous United States derived from NLDN measurements: 1993-2018, *Mon. Wea. Rev.*, **138**, 313-332, doi: 10.1175/MWR-D-19-0211.1

Koshak, W.J., Cummins, K.L., Buechler, D.E., Vant-Hull, B., Blakeslee, R.J., Williams, E.R., and Peterson, H.S., 2015: Variability of CONUS lightning in 2003-12 and associated impacts, *J. Appl. Met. Clim.*, **54**, 15-41, doi: 10.1175/JAMC-D-14-0072.1

Kurtzman, D. and Scanlon, B.R., 2007: El Niño-Southern Oscillation and Pacific Decadal Oscillation impacts on precipitation in the southern and central United States: Evaluation of spatial distribution and predictions, *Water Resources Res.*, **43**, doi: 10.1029/2007WR005863

Lawrence, M.G., 2005: The relationship between relative humidity and the dewpoint temperature in moist air: a simple conversion and applications, *Bull. Amer. Meteorol. Soc.*, **86**, 225-233, doi: 10.1175/BAMS-86-2-225

Liu, Y., Williams, E.R., Guha, A., Satori, G., Said, R.K., Virts, K.S., Lang, T.J., Zhu, Y., LaPierre, J., and DiGangi, E., 2024: Reduction in global lightning activity during the COVID pandemic, submitted manuscript available at https://authorea.com/users/579217/articles/1219080-reductionin-global-lightning-activity-during-the-covid-pandemic

Malloy, K., Tippett, M.K., and Koshak, W.J., 2023: ENSO and MJO modulation of U.S. cloud-to-ground lightning activity, *Mon. Wea. Rev.*, **151**, 3255-3274, doi: 10.1175/MWR-D-23-0157.1

Medici., G., Cummins, K.L., Cecil, D.J., Koshak, W.J., and Rudlosky, S.D., 2017: The intracloud lightning fraction in the contiguous United States, *Mon. Wea. Rev.*, **145**, 4481-4499, doi: 10.1175/MWR-D-16-0426.1

Mesinger, F., DiMego, G., et al. 2006: North American Regional Reanalysis. *Bull. Amer. Meteorol. Soc.*, **87**, 343–360, doi:10.1175/BAMS-87-3-343

Murphy, M.J., Cramer, J.A., and Said, R.K., 2021a: Recent history of upgrades to the U.S. National Lightning Detection Network, *J. Atmos. Ocean. Tech.*, **38**, 573-585, doi: 10.1175/JTECH-D-19-0215.1

Murphy, M.J., Said, R.K., Cramer, J.A., and Schulz, W., 2021b: May 2021 update to the central processing system of the U.S. National Lightning Detection Network, AGU Fall Meeting Abstracts, 2021, AE35A-1916.

Peters, J.M., Chavas, D.R., Lebo, Z.J., and Su, C-Y., 2024: Cumulonimbus clouds convert a smaller fraction of CAPE into kinetic energy in a warmer atmosphere, *J. Atmos. Sci.*, **81**, 1943-1961, doi: 10.1175/JAS-D-24-0006.1

Romps, D.M., Seeley, J.T., Vollaro, D. and Molinari, J., 2014: Projected increase in lightning strikes in the United States due to global warming, *Science*, **346**, 851-854, https://doi.org/10.1126/science.1259100

Romps, D.M., Charn, A.B., Holzworth, R.H., Lawrence, W.E., Molinari, J., and Vollaro, D., 2018: CAPE times P explains lightning over land but not the land-ocean contrast, *Geophys. Res. Lett.*, **45**, 12623-12630, doi: 10.1029/2018GL080267

Rudlosky, S.D., Goodman, S.J., and Virts, K.S., 2020: Lightning detection: GOES-R series Geostationary Lightning Mapper, ch. 16 of *The GOES-R Series*, https://doi.org/10.1016/B978-0-12-814327-8.00016-0

Said, R., 2017. Towards a global lightning locating system. *Weather (00431656)*, **72** (2).

Saunders, C., 2008: Charge separation mechanisms in clouds, *Space Sci Rev.*, **137**, 335-353, doi: 10.1007/s11214-008-9345-0

Taszarek, M., Allen, J.T., Brooks, H.E., Pilguj, N., and Czernecki, B., 2021: Differing trends in United States and European severe thunderstorm environments in a warming climate. *Bull. Amer. Meteorol. Soc.*, **102**, doi: https://doi.org/10.1175/BAMS-D-20-0004.1

Tippett, M.K. and Koshak, W.J., 2018: A baseline for the predictability of U.S. cloud-to-ground lightning. *Geophys. Res. Lett.*, **45**, 10719-10728, doi: https://doi.org/10.1029/2018GL079750

Williams, E.R., 2005: Lightning and climate: A review, *Atmos. Res.*, **76**, 272-287.

Williams, E. R., 2020: Lightning and climate change, ch. 1 of *Lightning Interaction with Power Systems: Volume 1 Fundamentals and Modelling* , A. Piantini, ed., London, U.K,, The Institution of Engineering and Technology.

Williams, E. and Stanfill, S., 2002: The physical origin of the land–ocean contrast in lightning activity, *Comptes Rendus Physique*, **3**, 1277-1292.

Williams, E., Rosenfeld, D., Madden, N., Gerlach, J., Gears, N., Atkinson, L., Dunnemann, N., Frostrom, G., Antonio, M., Biazon, B. and Camargo, R., 2002: Contrasting convective regimes over the Amazon: Implications for cloud electrification. *J. Geophys. Res.: Atmospheres*, **107** (D20), LBA-50.

[i] Corresponding author: Martin J. Murphy, Vaisala Xweather, 194 S. Taylor Ave., Louisville CO, 80027, USA, martin.murphy@vaisala.com